

A new decomposition of compound polarimetric targets

Armando Marino^a

^aThe University of Stirling, Natural Sciences, Stirling, Scotland, UK

Abstract

The use of polarimetric Synthetic Aperture Radar (PolSAR) has the capability to improve detection and bio-physical parameters extraction in many remote sensing applications compared to the use of a single polarisation channel. The scattering matrix or the scattering vector allow to analyse the polarimetric information of targets. Unfortunately, when dealing with distributed targets, speckle introduces a statistical variation on the visible polarimetric behaviour and we need statistical tools. Generally the adopted solution is to extract second order statistics building a covariance matrix. Unfortunately, the covariance matrix formation as an averaged outer product of scattering vectors by themselves impose constraints on the power distribution in the polarimetric space (this is the shape of the surface drawn by the quadratic forms). The surface is forced to be an ellipsoid. In this work we show how such forcing can produce a loss of information. We propose an alternative way to decompose the partial target into a sum of low entropy components which does not require indiscriminate pre-averaging. To demonstrate its usefulness we use both Monte Carlo simulations and real quad-pol data. We compare the results of the proposed decomposition with the ones obtained by the Cloude-Pottier decomposition and show how the use of indiscriminate averaging can produce bias in the retrieval of the original scattering mechanisms.

1 PolSAR

In the following, a very brief introduction to Pol-SAR is proposed with the only purpose of presenting the mathematical formalism exploited in the following. A single target has a fixed polarization in time/space and we can characterize it using the scattering (Sinclair) matrix or equivalently a scattering vector \underline{k} [1]. It is possible to define a projection vector as a normalized vector $\underline{\omega} = \frac{\underline{k}}{\|\underline{k}\|}$. This is often referred to as scattering mechanism (SM), however in the following we refer to SM as the process producing scattering vectors. The targets observed by a SAR system are generally not single SMs, but a combination of different SMs which we refer to as a partial target. In order to characterize a partial target the single scattering matrix is not sufficient since these are stochastic processes and second order statistics need to be considered. To most common way to do this, is by extracting the target covariance matrix as $C = \langle \underline{k} \underline{k}^{*T} \rangle$, where $*$ stands for conjugate, T for transpose and $\langle \cdot \rangle$ is the finite averaging operator [1]. In this work, we propose an alternative to this formalism.

1.1 Decompositions

Polarimetric data allow to decompose the backscattering into different components each one coming from a specific SMs. In the covariance matrix formalism, the power coming from a SM, can be written using a quadratic form as $\underline{\omega}^{*T} [C] \underline{\omega}$. In the following, we use the Pauli decomposition to represent the scattering vector ($\underline{k}_p = \frac{1}{\sqrt{2}} [HH + VV, HH - VV, 2HV]^T$). Incoherent decompositions are the ones more appropriate for distributed targets and they use the covariance matrix as starting point. One of the most notorious decompositions is the Cloude-Pottier which is a diagonalisation of the covariance matrix and a parameterisation of the eigenvectors [1, 2]. The diagonalisation is looking at the shape formed by the quadratic form $\underline{\omega}^{*T} [C] \underline{\omega}$ by varying $\underline{\omega}$ and extract its maxima. The covariance matrix is Hermitian, which is handy since it returns a convex optimisation, however this forces the shape of the power surface to be an ellipsoid [3]. This means that the eigenvectors are forced to be orthogonal, no matter what targets are actually present in the scene. The Cloude-Pottier decomposition is used in the following because, up to our knowledge, it is the decomposition that best characterise the shape of the $\underline{\omega}^{*T} [C] \underline{\omega}$ surfaces after indiscriminate average and therefore, in our opinion, is the one that most closely represents the physics behind the scattering. Any other incoherent decomposition using $[C]$ would suffer from this artifact, since the issue is with the formation of $[C]$ itself.

© 2021 IEEE. Personal use of this material is permitted. Permission from IEEE must be obtained for all other uses, in any current or future media, including reprinting/republishing this material for advertising or promotional purposes, creating new collective works, for resale or redistribution to servers or lists, or reuse of any copyrighted component of this work in other works.

2 Compound decompositions

2.1 Compound targets

The constraint on the shape of $\underline{\omega}^{*T}[C]\underline{\omega}$ is a direct consequence of the linearity of Maxwell equations (i.e. superposition of waves). If we have SMs homogeneously mixed in each of the resolution cells, then the vectors coming from each pixels will show this mix and indiscriminate averaging will produce some extra-mixing that is not affecting much the result. However, indiscriminate averaging introduces significant errors in several situation as shown in the following.

In this work we propose a methodology that can improve drastically the situations, where targets can be seen as a collection of several SM each separable at pixel level. Here we call these type of targets as Compound targets. This is the case of targets where each cell is relatively dominated by a typology of target. Urban areas or extended artificial targets (e.g. ships) are very good example of this type. Forests with gaps (they may have that some pixels are clearly surface scattering, some clearly double bounce and other volume) can also provide such behaviour. As a rule of thumb, the higher is the resolution, the more likely is that we have the appearance of compound targets.

Here we propose a new way to process PolSAR data which allows to separate the compounds without forcing orthogonality between them. It is important to keep in mind that the orthogonality constraint is not forced by the Cloude-Pottier processing of $[C]$, but by the formation of $[C]$ itself. The outer product of a vector by itself is a form of autocorrelation and autocorrelations must be symmetric. If we plot the power (i.e. quadratic form) for each projection vector $\underline{\omega}^{*T}[C]\underline{\omega}, \forall \underline{\omega} \in \mathbb{C}^3$, the shape is a 3D ellipsoid. As such it will have one major, one minor and one middle axis. The eigenvectors of the Cloude-Pottier decomposition are able to identify these axes. On the other hand, we do not expect that nature arrange SM so that they are orthogonal to each other. SM can have any directions in the 3D complex space, it is their indiscriminate average that produce an ellipsoid (no matter what are the initial directions of the SMs).

2.2 Finding the compounds

In this section we present the methodology to extract the SM forming the compound. Scattering vectors in an image can be seen as a tensor field.

We can separate the image in searching windows as it is done by boxcar speckle filters. Window size of 7×7 or larger could be used. In each box, we will have a tensor field with N vectors (e.g. 49 vectors for a box 7×7). The order of these vectors in the box is not important and in the following we will use a 1-D formalism to represent them (as if they would be arranged along a line). Due to the fact that the absolute phase of the scattering vector is related to the distance, vectors will be pointing in every directions regardless of the type of target present. The first step is to remove dependency to the distance by multiplying the vector by the scalar $e^{j\phi}$, where $\phi = \angle k_1$ and k_1 is the first component of \underline{k} .

After this correction, some of the vectors will point in similar directions. This is because they may be produced by the same scattering mechanism. In case of a distributed single target, all the vectors will be perfectly aligned (they will lead to a rank one covariance matrix). If we have two SMs, we will have some vectors that points in one direction and some in another. This two directions are not forced to be orthogonal (they can be any direction), but they span a plane. Interestingly if they are uniformly mixed inside each resolution cell, or if they are indiscriminately averaged with each other they will lead to a rank 2 matrix with a quadratic form (i.e. power) drawing an ellipse.

Speckle will affect the intensity of these vectors, but their direction is pretty much unchanged and it depends on the purity of the scattering mechanism. If a scattering mechanism is well defined, then the speckle will not change the direction of the vector at all. We can think of this as a collection of polarisers. If we change the distribution of the polarisers the total intensity will change but the total field will still have the same polarisation of each of the polarisers. If the polarisation state of each of the SM is not well defined, than the vector direction may change a bit in each pixel. These reasoning comes as straight consequence of the physical reasoning that lead to the ellipsometry studies of wave polarisation [4]. When converted to target polarimetry this means that a single (non moving target) is reflecting a polarised wave, plus a depolarised component due to noise. Delving more on this similarity is not the purpose of this abstract, and therefore we leave it to the paper version.

Here we will assume that a SM is polarised enough to produce a set of vectors in the tensor field that points to a similar region of the space. An optimisation is performed that

1. For each area considers the vector with bigger magnitude.
2. Performs a normalised inner product with the rest of the tensor field. This inner product is equal to the cosine of the angle between the two vectors.
3. If the angle is smaller than θ_T then it performs an outer product and produces a covariance matrix for those points, if is bigger it leaves the pixel unprocessed. In our experiment we selected $\theta_T = 30^\circ$. A mask M is created where all the processed pixels are set to 1.
4. The process 1, 2 and 3 is repeated after removing the set of pixels in the previous mask M .

5. The process is terminated either if all the pixels are associated to a covariance matrix or if a set number of covariance matrices is reached, N_T . N_T is the maximum number of target compounds we want to retrieve.

In this experiments, we set $N_T = 5$, but a larger number of targets could be selected (in that case it may be convenient to have a smaller θ_T). This procedure singles out the different compounds forming the target and therefore it could be used to decompose the full covariance matrix. Since each of the compounds may have a different number of pixels in the box, it is easier to talk about total power from a compound more than averaged power, because they contribute differently to the total target power. For this reason, in the following we did not perform the division by the number of pixels, and we talk about total power more than averaged power. However, the average can be easily implemented if required.

Since we use only N_T (non-orthogonal) SM, we are not sure we will be covering the total power coming from the tensor field in the box (i.e. we are not sure if we will miss out some of the vectors in the field). Therefore, the partial target we reconstruct with N_T SM (and without indiscriminate averaging) is not necessarily the full target. Interestingly the amount of reconstructed power is an indicator of the number of SM in the box. A completely unpolarised field is likely to have lots of unreconstructed power. As showed in the following, we can build entropy measures of such unreconstructed portion and help classify phenomena as volume scattering.

In a more compact way the reconstruction is done as:

$$[\hat{C}]_R = \sum_{i=1}^{N_T} [\hat{C}]_i = \sum_{i=1}^{N_T} \left[\sum_{j=1}^{N_j} \underline{k}_j \underline{k}_j^{*T} \right] \quad (1)$$

$$\forall j: \frac{\underline{k}_i^{*T} \underline{k}_j}{\|\underline{k}_i\| \cdot \|\underline{k}_j\|} < \theta_T, \|\underline{k}_i\| > \|\underline{k}_j\|, M_j = 0. \quad (2)$$

$[\hat{C}]_R$ is the reconstructed covariance matrix (not divided by the number of pixels), $[C]_i$ is the covariance matrix for the pixel i , θ_T is the angle selected to separate different targets (we selected 45°) and M_j is the mask which is 0 if the pixels has not been used before or 1 if it has been used. It is clear that $[\hat{C}]_R$ can be easily normalised and converted into a $[C]_R$.

2.3 Expected theoretical behaviour of algorithm

Given the following three assumptions we expected the following behaviour:

2.3.1 Single SM

The tensor field for a single target can be represented either by a very dominant vector (with length many order of magnitude larger than others) or by a series of vectors all pointing at the same direction. Due to noise and other non-ideality the depolarisation of these waves will produce some slight changes in directions. The procedure will return a single covariance matrix detecting 1 target component. The Cloude-Pottier entropy of that matrix will be proximal to zero (but not zero).

2.3.2 Small number of SM

If the partial target is composed by a limited number of targets, separated in different pixels, the procedure will be able to pick each of the compounds forming the partial target. It will return several covariance matrices, each one related to a component of the total target. The components can be more than 3 and they are not forced to be orthogonal with each other.

2.3.3 Depolarised targets and uniform mixing

If the partial target is composed by different polarimetric targets which are very depolarised for some reasons or they are quite uniformly mixed in each resolution cell, the algorithm will not be able to find a limited amount of components. The subresolution mixing will produce again a ellipsoid, the final shape of the tensor field power will resemble the ellipsoid itself and there should not be any advantages using the compound formalism. These type of targets are the ones that return high entropy and neither the Cloude-Pottier or the proposed decomposition are able to unpick the SM in within the resolution cell. The output of the algorithm will be N_T components with not very dissimilar power. If we consider the power explained by the components and the total power we can see that the reconstruction is not good and a significant amount of power is missing. This is also obtained if we calculate the entropy of the compound power. In that case we can classify the target as highly depolarised.

3 Monte Carlo Simulation

Here we perform Monte Carlo (MC) simulations to validate that we can decompose compound targets into components even if these are not orthogonal to each other.

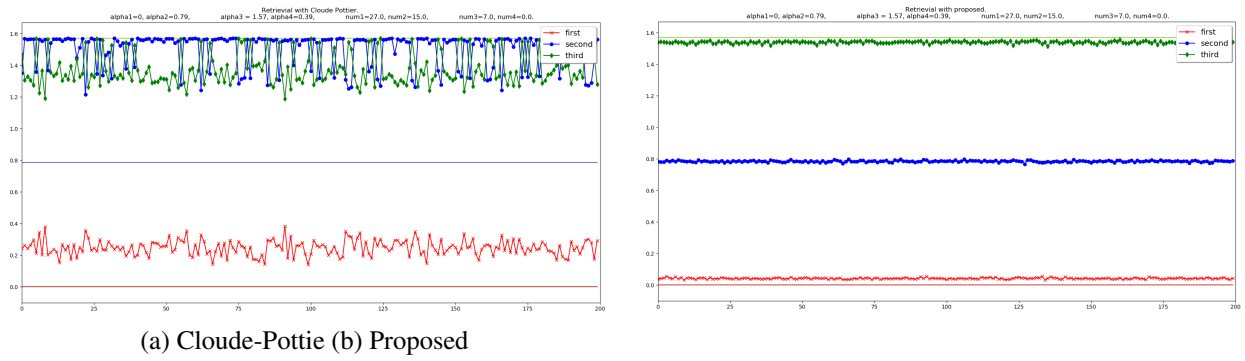


Figure 1 Monte Carlo simulations for reconstruction of 3 targets non-orthogonal to each other: (a) α angle of Cloude-Pottier eigenvectors (b) α angle of proposed decomposition. Solid line actual value, symbols reconstruction. Box size: 7×7 .

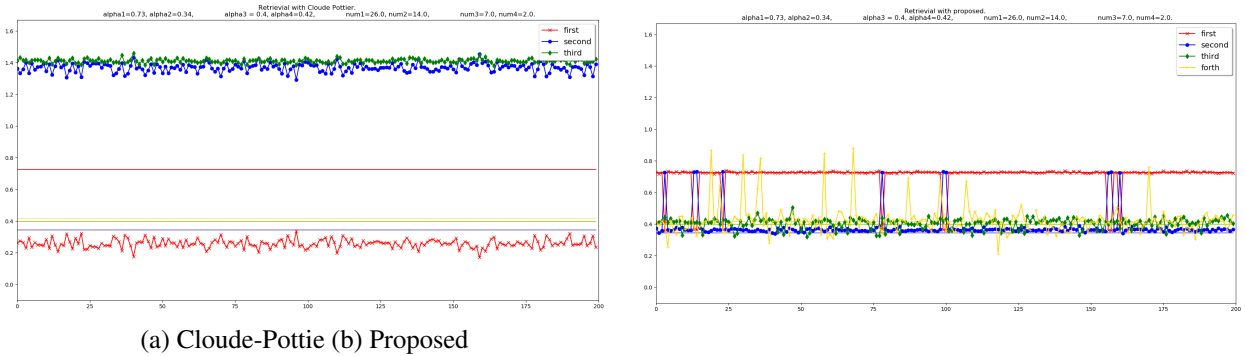


Figure 2 Monte Carlo simulations for reconstruction of 4 targets non-orthogonal and randomly: (a) α angle of Cloude-Pottier eigenvectors (b) α angle of proposed decomposition. Solid line actual value, symbols reconstruction. Box size: 7×7 .

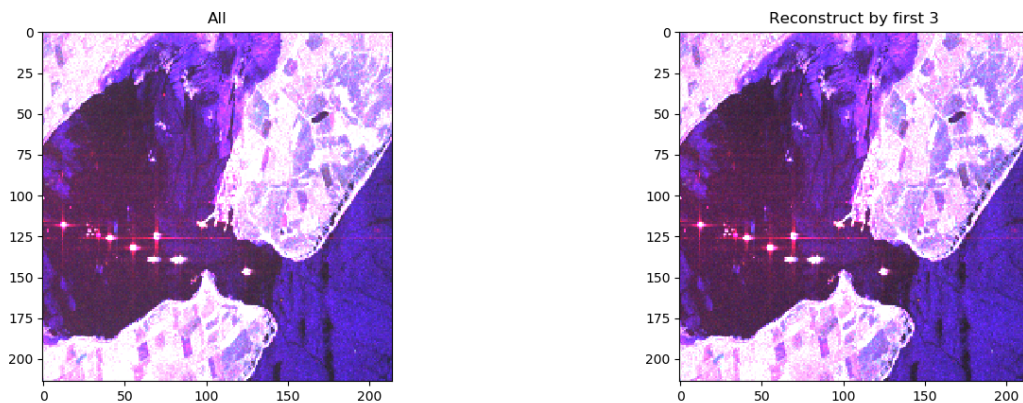
1. We generate 3-D circular complex Gaussian unitary vectors.
2. These vectors are then coloured using low entropy covariance matrices representing the SM (where the main eigenvalue is 1000 time bigger than then second). This is a more realistic solution that using rank one matrices since it tries to simulate the depolarisation of the target components.
3. We then set the number of pixels in the box that presents each of the SMs. To make the analysis simpler we set the mean backscattering of each of the targets pixel as the same (i.e. all the vectors have the same length). This only helps interpretation when ranking the components, but it does not affect generality.

Note that the output of the simulation are scattering vector (coloured by a covariance matrix) and not covariance matrices themselves. We are therefore simulating coherent and not incoherent data. For lack of space only two scenarios are shown in this abstract.

In Figure 1 we simulated a partial target composed by 3 SM that are not orthogonal to each other. To test the retrieval of the SM we are plotting here the Cloude-Pottier α angle (i.e. arcosine of magnitude of first component of Pauli scattering vector). Solid lines are actual values while symbols are reconstructions. It can be seen that the SM are better estimated by the proposed method. The use of an indiscriminate covariance matrix has problem due to the constraint on having orthogonal components.

In Figure 2 we simulated a partial target composed by 4 SMs that are randomly oriented. They are obviously non orthogonal to each other. The diagonalisation is not able to deal with this type of targets producing only three eigenvectors with wrong estimation of SMs. The proposed methodology is able to separate the components more properly. It is also interesting to notice that in mis-estimations it is often the case that the ranking of the SM is different but the value of alpha is still correct (e.g. the second is estimated as the first). This is due to the fact that speckle affects largely the amount of power of each single component and this may impact the ranking of the SM.

It is not showed here, but both methodologies equally fails significantly when each pixels is obtained by a similar mixture of different scattering mechanisms. Interestingly, they both pick reasonably well the dominant SM, but largely mis-estimate the others. This is because each of the vectors of the tensor field is not representative anymore of the SMs, but a linear combination of those. More experiments have been carried out to evaluate selection of θ_T , N_T , block size and



(a) Pauli RGB

(b) Pauli RGB reconstructed after decomposition

Figure 3 Pauli RGB of the area of interest: (a) Original RGB (b) Reconstructed RGB. Box size: 7x7.

different combination of SM. These will be presented at the conference.

4 Real Data analysis

In this section we test the algorithm over quad-pol real data.

4.1 Data

Here only one RADARSAT-2 dataset is presented, but at the conference we will also present results with ALOS-2 data. The quad-pol RADARSAT-2 data were acquired in Scotland, Nigg Bay in 2018. Figure 3.a presents the Pauli RGB image of a portion of the image under analysis. This is a bay and the bright targets are infrastructure (i.e. platforms) for building oil rigs.

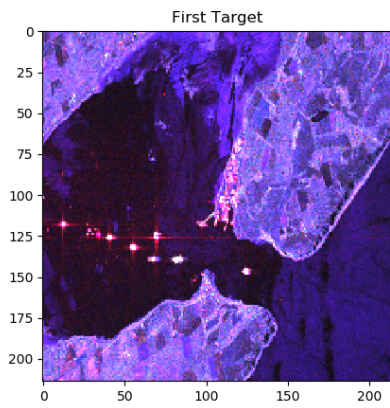
4.2 Results

The proposed algorithm is run on the data and the first two components are presented in Figure 4 as Pauli RGB images. This is, the covariance matrix of the component is represented in Pauli format and visualised as an RGB. This allows us to interpret the components using the Pauli RGB decomposition. The two images are scaled at the same way (each Pauli component in each RGB is scaled using the same maximum and minimum), so that images are comparable. Interestingly, the dominant scattering mechanism seems to be either a surface (blue over sea and several fields) or horizontal dihedral (red over several platforms, town and some fields). The second is also reddish with some hints of green as well. In order to have indication on the depolarisation of the targets and have an indication on how many scatterers are present, we can evaluate a compound entropy as the entropy of the first N_T SM. Interestingly the sea has a very low entropy (almost unitary), while areas of low wind and slicks have a high entropy. As a comparison we can plot the Cloude-Pottier entropy in Figure 4.c. The two images of entropy are in agreement, however, the compound entropy seems to have a higher contrast where places dominated by a single SM appear having a lower entropy.

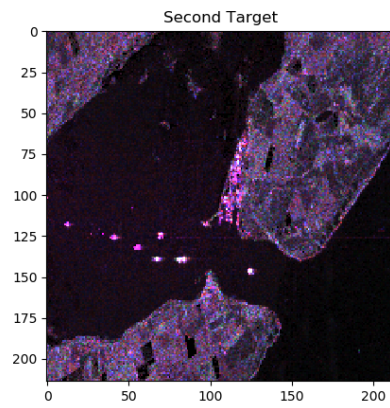
5 Conclusions

In this work, we proposed a new methodology to deal with distributed targets presenting speckle. Indiscriminate averaging inside the test cell forces the shape of the surface produced by the matrix quadratic form to be an ellipsoid. This is appropriate only in case of fully developed speckle. In this work, we propose a different solution to extract second order statistics which is not based on indiscriminate averaging.

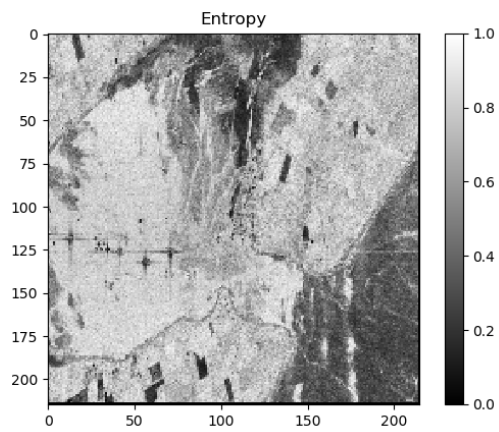
We propose an alternative way to decompose the partial target into a sum of low entropy components which does not require indiscriminate pre-averaging. To demonstrate its usefulness we used both Monte Carlo simulations and real quad-pol data. The comparison of the proposed decomposition with the ones obtained by the Cloude-Pottier decomposition showed how the use of indiscriminate averaging can produce bias in the retrieval of the original scattering mechanisms.



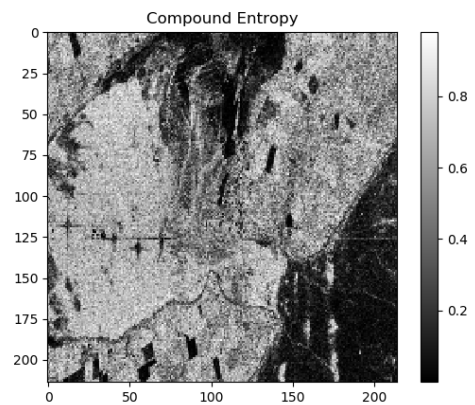
(a) Pauli RGB First



(b) Pauli RGB Second



(a) Pauli RGB Third



(b) Compound entropy

Figure 4 Pauli RGB of the retrieved targets: (a) Scattering mechanisms for the dominant target (b) Second target; (c) Cloude-Pottier entropy; (d) Compound entropy. All images are scaled in the same way. Box size: 7x7.

6 Acknowledgements

Data were kindly provided by MDA and CSA. RADARSAT-2 data and products ©, Maxar Technologies Ltd (2018-2019), All rights reserved. RADARSAT is an official trademark of Canadian Space Agency. RADARSAT-2 data were provided courtesy of MDA and Canadian Space Agency under the SOAR project 5440.

7 Literature

- [1] Polarisation: Applications in Remote Sensing, Cloude, S. R., Oxford University Press, Oxford, UK, 2009
- [2] An Entropy Based Classification Scheme for Land Applications of Polarimetric SAR, Cloude, S. R. and Pottier, E., IEEE Transactions on Geoscience and Remote Sensing, 1997, 68-78, 35.
- [3] Lie Groups in EM Wave Propagation and Scattering, Cloude, S.R., Chapter 2 of Electromagnetic Symmetry, C Baum and H N Kritikos, 91-142, Taylor and Francis, Washington, USA, ISBN 1-56032-321-3, 1995.
- [4] Polarized Light, D. H. Goldstein, CRC Press, 2011.